CrossMark

Experimental study on the heat transfer and flow properties of γ-Al₂O₃/water nanofluid in a double-tube heat exchanger

Behrouz Raei[1] · Farhad Shahraki[1] · Mohammad Jamialahmadi[2] ·
S. M. Peyghambarzadeh[3]

Abstract Double-tube heat exchanger is primarily adapted to high-temperature, high-pressure applications due to their relatively small diameters. An experimental study performed to investigate the effects of Al₂O₃/water nanofluid on the hydrodynamics and convective heat transfer of a counter flow double-tube heat exchanger. The nanofluid was used as hot fluid and passed through the inner tube of the heat exchanger considering fully developed turbulent flow regime. Experiments were conducted at the nanofluid flow rates of 7, 9, and 11 L min⁻¹, nanofluid inlet temperatures of 45, 55, and 65 °C, and dilute nanoparticle concentrations of 0.05 and 0.15 vol%. Local convective heat transfer coefficient in double-tube heat exchanger has been measured experimentally for the first time. Results showed that nanofluids had higher Nusselt number than pure water. Also, the Nusselt number increased by increasing particles volume fraction, flow rate as well as temperature of nanofluid. However, increasing the convective heat transfer coefficient of the nanofluids was not sensible with increasing the concentration. In addition, the ratio of the heat transfer coefficient of nanofluid to that of the base fluid decreased by increasing Reynolds number. Adding γ-Al₂O₃ nanoparticles to the base fluid increased the friction factor. In this study, the greatest enhancement in the heat transfer coefficient and the friction factor obtained at 0.15 vol% concentration of nanoparticles which were 23 and 25 %, respectively.

Abbreviations

CNT	Carbon nanotube
C_p	Specific heat (J K⁻¹ °C⁻¹)
DWCNTs	Double-walled carbon nanotubes
D_B	Brownian diffusion coefficient
D_T	Thermophoresis diffusion coefficient
Exp	Experimental
EG	Ethylene glycol
f	Friction factor
h	Heat transfer coefficient (W m⁻² K⁻¹)
h	Hour
ID	Inner diameter (mm)
k	Thermal conductivity (W m⁻¹ K⁻¹)
L	Liter
L	Length of the test section (m)
N_{BT}	Ratio of the Brownian to thermophoretic diffusivities
Nu	Nusselt number
P	Pressure (Pa)
PC	Personal computer
Pe	Peclet number
Pr	Prandtl number
PID	Proportional–integral–derivative
PVC	Polyvinyl chloride
q	Heat transfer rate (kW)
Q_h	Volume flow rate of hot water (L min⁻¹)
Q_c	Volume flow rate of cooling water (L min⁻¹)
Ra	Rayleigh number
Re	Reynolds number

✉ Farhad Shahraki
fshahraki@eng.usb.ac.ir

[1] Department of Chemical Engineering, University of Sistan and Baluchestan, Zahedan 98164-161, Iran

[2] Petroleum Engineering Department, Petroleum University of Technology, Ahwaz, Iran

[3] Department of Chemical Engineering, Mahshahr Branch, Islamic Azad University, Mahshahr, Iran

TEM	Transmission electron microscopy
T	Temperature (°C)
V	Volt
vol	Volume
x	Axial distance

Greek symbols

φ	Volume fraction
ε	Roughness (m)
μ	Viscosity (Pa s)
ρ	Density (kg m^{-3})
Δ	Difference

Subscripts

av	Average
b	Bulk
bf	Base fluid
c	Cold
e	Equivalent
h	Hot
i	Inner
nf	Nanofluid
o	Outer
p	Particle
w	Wall
x	Local

Introduction

Conventional heat transfer properties of fluids are a major obstacle to the development of effective and compact heat transfer equipment. Heat transfer fluids are regularly used in industries including water, ethylene glycol, propylene glycol, and engine oil that generally have low heat transfer coefficient. One way to increase heat transfer efficiency is improving thermal conductivity of working fluid, which this goal could be achieved by adding nano-sized particles to the base fluid. This type of fluid was called nanofluid for the first time by Choi [1]. In industrial thermal design to reduce capital cost, heat transfer area should be reduced which can be obtained by increasing the heat transfer coefficient. Nanofluids as heat transfer fluid have a bright future because of better stability in comparison with microfluids and increase the thermal conductivity even at low concentrations [2–8]. Numerous experimental studies have been conducted to investigate the thermal properties and hydrodynamics of the nanofluids that majority of them have reported positive effect of nanofluids on the heat transfer coefficient.

Xuan and Li [9] measured the heat transfer coefficient of Al_2O_3/water nanofluid and reported 35 % enhancement at

2 vol% of alumina nanoparticles. Yu et al. [10] obtained experimental heat transfer data for water/EG (45/55 vol%) and alumina nanoparticles. They observed that at 1 and 2 vol% of nanoparticle, the rate of heat transfer increased 57–106 %, at $Re = 2000$. Wen and Ding [11] studied the heat transfer in laminar flow regime under constant heat flux boundary condition using Al_2O_3/water nanofluid. They have reported that increasing the Reynolds number and concentration of nanoparticles, especially at the entrance region, increases the heat transfer coefficient of nanofluid. Peyghambarzadeh et al. [12] studied the heat transfer coefficient of Al_2O_3/water nanofluid in a car radiator. They observed the heat transfer enhancement of about 45 % compared with pure water. An experimental study was conducted to clarify the forced convective heat transfer coefficient and pressure drop of water-based nanofluid including MWCNT flowing through a horizontal circular tube by Hosseinpour et al. [13]. They have reported a significant increase in the convective heat transfer coefficient with the addition of the MWCNT. Also, the convective heat transfer coefficient increased with increasing the nanofluid concentration and Reynolds number. Tarighaleslami et al. [14] implemented CuO/water nanofluid as an intermediate fluid of heat recovery loop in a large dairy factory. They showed that CuO/water nanofluid has significant effect on increasing heat recovery rate and decreasing heat transfer area in different plants.

The effect of magnetic field on heat transfer enhancement and friction factor of Fe_3O_4/water nanofluid was experimentally investigated by Hosseinzadeh et al. [15]. According to the obtained results, the Nusselt number has improved with an increase in Reynolds number and concentration of nanopowders. The same result was also observed with increasing the magnetic field strength. Moreover, the friction factor of nanofluids was more than that of pure water due to the presence of solid nanoparticles. Esfe and Saedodin [16] experimentally studied the thermal conductivity, dynamic viscosity, and Nusselt number of turbulent forced convection of MgO/water nanofluid in a circular straight pipe. The pure water and nanofluid with the nanoparticle volume fraction of 0.005, 0.01, 0.015, and 0.02 and the nanoparticles diameter of 60, 50, 40, and 20 nm were considered. The experimental results indicated that the existence of the nanoparticles in the pure water with all considered values of the nanoparticles volume fraction and diameter motivated the rate of heat transfer to increase. Bahiraei [17] numerically applied the Euler–Lagrange approach to investigate heat transfer characteristics of the CuO/water nanofluid in a straight tube. The results revealed significant increment of heat transfer for the nanofluid in comparison with the pure water. For instance, at $\varphi = 0.3$ % and $\varphi = 3$ %, the amounts of average heat transfer enhancement were about

6 and 14 %, respectively. An experimental study was carried out to investigate the performance of horizontal double-tube counter flow heat exchanger by El-Maghlany [18]. The heat exchanger performance was tested with Cu nanoparticles addition in the coolant water and the rotation of the inner tube. The influence of the flow Reynolds number and the solid volume fraction in addition to the rotation speed of the inner tube were investigated. Results demonstrated a remarkable enhancement in the rate of heat transfer due to the nanoparticles addition as well as the inner tube rotation.

Malvandi and Ganji [19] studied a theoretical investigation of the laminar flow and convective heat transfer of alumina/water nanofluid inside a circular microchannel in the presence of a uniform magnetic field. The results indicated that nanoparticles migrate from the heated walls (nanoparticles depletion) toward the core region of the microchannel (nanoparticles accumulation) and construct a non-uniform nanoparticles distribution. The ratio of the Brownian to thermophoretic diffusivities (N_{BT}) had relatively significant effects both on the distribution of the nanoparticles and the convective heat transfer coefficient of nanofluids. It was further observed that for smaller nanoparticles, the nanoparticle volume fraction is more uniform and abnormal variations in the heat transfer rate vanish. Also, Malvandi et al. [20] numerically studied thermal performance of hydromagnetic alumina/water nanofluid inside a vertical microannular tube considering different modes of nanoparticle migration. A theoretical investigation of the laminar flow and convective heat transfer of Al₂O₃/water nanofluid inside a horizontal annulus with a streamwise moving inner cylinder conducted by Malvandi and Ganji [21].

Some of experimental studies are cited in Table 1 to investigate the thermal performance of nanofluids in double-tube heat exchangers.

Despite vast researches on thermal and hydrodynamic properties of nanofluids, a large inconsistency could be observed in results. One of the reasons is the use of thermophysical properties particularly viscosity and effective thermal conductivity of nanofluids which is an important factors in calculating Reynolds, Prandtl, and Nusselt numbers. Another reason for this inconsistency could be attributed to the stability of the nanofluid and variety of test methods which are very important in turbulent flow regime. Sergis and Hardalupas [31] statistically reported that most of previous studies showed a small increase in heat transfer, 11 % showed deterioration of heat transfer coefficient, and 3 % did not show any increase. Those articles that implemented nanofluid and indicated trivial increase or even decrease in heat transfer coefficient are reviewed.

Fotukian and Esfahani [32] studied the turbulent convective heat transfer with γ-alumina/water nanofluid in a circular pipe. Their results indicated that increasing the concentration of nanoparticles from 0.054 to 0.2 vol% has no great effect on the heat transfer changes. Ni et al. [33] examined thermal and flow properties of alumina/water nanofluid in turbulent regime. The results showed that convective heat transfer coefficient (h), Nusselt number (Nu), and Rayleigh number (Ra) are reduced with increasing the nanoparticles volume fraction. In addition, at certain conditions, heat transfer of alumina nanofluids is significantly less than water. Duangthongsuk and Wongwises [24] studied the thermal and rheological impact of TiO₂/water nanofluid in a double-tube heat exchanger at the concentration of 0.2–2 vol%. Their results showed that the heat transfer coefficient of nanofluid at the concentration of 2 vol% is almost 14 % less than based fluid at same conditions. Peyghambarzadeh et al. [34] studied the heat transfer performance of the automobile radiator. Copper oxide (CuO) and iron oxide (Fe₂O₃) nanoparticles are added to the water at three concentrations 0.15, 0.4, and 0.65 vol%. Results demonstrated that both nanofluids show greater overall heat transfer coefficient in comparison with water up to 9 %.

According to experimental studies, most studies carried on circular smooth tube with constant heat flux boundary condition and/or fixed surface temperature. Therefore, thermal and flow properties of nanofluids in a double-tube heat exchanger are less studied. Particularly, distribution of local convective heat transfer coefficient in double-tube heat exchangers is unclear. As a result, in the present study, thermal and hydrodynamic properties of much diluted γ-alumina/water nanofluid are studied in fully developed turbulent flow regime in a double-tube heat exchanger.

Experimental

Preparation of the nanofluid

Preparation of nanofluids is the first key step in experimental studies using nanoparticles to improve the thermal efficiency of fluids. Two methods including single-step and two-step exist for nanofluid production. As the nanoparticles are commercially available, many researchers used two-step procedure for preparing nanofluids. Specification of γ-alumina nanoparticles (purchased from Nanosany Co.) is shown in Table 2. A transmission electron microscope (TEM) was used to approximate the size of the primary nanoparticles. As shown in Fig. 1, it is clear that the primary shape of nanoparticles is approximately spherical. This method is commonly used by a wide range of researchers [24, 35, 36].

In the two-step method, providing stable nanofluid is a challenge. Various methods such as changing in pH of the

Table 1 Summary of the experimental investigations on heat transfer in double-tube heat exchanger with nanofluids

References	Base fluid	Nano particle/mean diameter	Volume fraction %	Dimension	Flow regime/ Re	Maximum enhancement of heat transfer coefficient
Esfe et al. [22]	Water	COOH–functionalized DWCNTs	0.01, 0.02, 0.05, 0.1, 0.2 and 0.4	Inner tube ID: 7.05 mm Outer tube ID: 37.9 mm L:110 cm	Turbulent	32 % at $\varphi = 0.4$ %
Darzi et al. [23]	Water	Al_2O_3/20 nm	0.25, 0.5 and 1	Inner tube ID: 8.1 mm Outer tube ID: 150 mm L:220 cm	5000–20,000	20 % in Nu number at $\varphi = 1$
Duangthongsuk et al. [24]	Water	TiO_2/21 nm	0.2, 0.6, 1, 1.5 and 2	Inner tube ID: 8.13 mm Outer tube ID: 27.8 mm L:150 cm	Turbulent	26 % at $\varphi = 1$ %
Zamzamian et al. [25]	EG	Al_2O_3/20 nm CuO/20 nm	0.1, 0.5 and 1 (mass%) 0.1, 0.3, 0.5, 0.7 and 1 (mass%)	Inner tube ID: 12 mm Outer tube ID: 50.8 mm L:70 cm	Turbulent	26.2 % at $\varphi = 1$ % 37.2 % at $\varphi = 1$ %
Esfe et al. [26]	Water	MgO/40 nm	0.0625, 0.125, 0.25, 0.5 and 1	L:111 cm	Turbulent	35.93 % at $\varphi = 1$ %
Chun et al. [27]	Transformer oil	Al_2O_3/7, 27, 43 nm	0.25 and 0.5	Inner tube ID: 6.35 mm Outer tube ID: 12.7 mm L:500 cm	Laminar	25 % at $\varphi = 0.5$ %
Aghayari et al. [28]	Water	γ-Al_2O_3/20 nm	0.1, 0.2 and 0.3	Inner tube ID :6 mm Outer tube ID: 14 mm L:120 cm	15,000–28,000	12 % at $\varphi = 0.3$ %
Khalifa et al. [29]	Water	γ-Al_2O_3/10 nm	0.25, 0.5, 0.75 and 1	Inner tube ID: 20 mm Outer tube ID: 50 mm L:76 cm	Turbulent	22.8 % at $\varphi = 1$ %
Sarafraz et al. [30]	EG (50 %) Water (50 %)	Ag/40–50 nm	0.1, 0.5 and 1	Inner tube ID: 6.35 mm Outer tube ID: 12.7 mm L:240 cm	Laminar and Turbulent	67 % at $\varphi = 1$ %

nanofluid, addition of surface activators (surfactants), and ultrasonic vibration are used to achieve stable nanofluids. In this study, nanofluid with the concentrations of 0.05 and 0.15 of vol% was prepared. A certain amount of γ-alumina nanoparticle is weighed (accurate to three decimal places) and added to distilled water as a based fluid. After half an hour of mixing with magnetic stirrer, fluid was placed in an ultrasonic vibrator (BANDELIN Company with a power of

Table 2 Specification of nanoparticle used in this study

Nanoparticle	Aluminum oxide/γ
Average particle size/nm	20
Purity	>99 %
Density/kg m^{-3}	3890
Color	White
Morphology	Nearly spherical
Specific area/m^2 g^{-1}	>138
Specific heat/J kg^{-1} K^{-1}	880
Thermal conductivity/Wm^{-1} K^{-1}	46
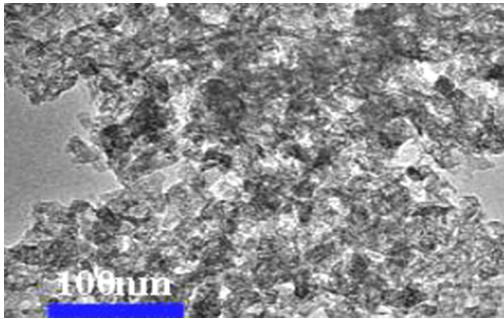
Fig. 1 Image of TEM nanoparticles used in this study
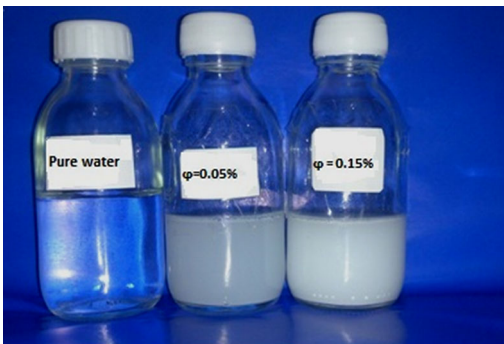
Fig. 2 Samples of prepared nanofluid after 24 h

240 kW and frequency of 35 kHz) for 3 h. Figure 2 shows the nanofluid stability after 24 h.

The repeatability was investigated during tests. Some tests repeated randomly at different times, and it was determined that there is very little difference between them. This means that with the passage of time, no changes occurred in test results and it can be concluded that the situation of nanofluid is steady in terms of stability. Over time, random sampling was done from certain part of the experimental setup. The samples were then dried in the oven, and its mass was measured to determine the concentration. The results showed that little difference existed between initial concentration and subsequent concentration.

So, all these reasons show that nanofluids homogeneously distributed in the heat exchanger and situation of nanofluid is steady in terms of stability.

It should be noted that no surfactant was used during the preparation of nanofluid due to the changes of its thermophysical properties. In addition; sedimentation of nanoparticles has less importance in the turbulent flow regime because of the higher imposed shear which breaks down the possible agglomerated particles. Therefore, turbulent flow regime helps to produce stable nanofluid in the experiment. This point of view was presented by Nasiri et al. [37].

Experimental

Schematic view and realistic photograph of the experimental setup are shown in Fig. 3a, b. The test loop consists of two reservoir tanks, a heater, a digital thermostat controller with PID controller, two flow meters, one flange, temperature sensors, two centrifugal pumps, data logger, control box, a U-shaped manometer, metal valves for opening and closing of flow passes, and a personal computer. The test section includes a double-tube heat exchanger that composed of two concentric tubes. The hot fluid (nanofluid) passes through the inner tube which is made of stainless steel (316 SS) with 12.7 mm inner diameter and 6 mm thickness. The cold fluid (distilled water) passes through the outer tube that surrounds the inner tube and is made of carbon steel with 63.5 mm inner diameter and 6 mm thickness. The total length of the test section is 60 cm. According to the following equation: $\left(\frac{L_e}{D} \sim 4.4\,Re^{\frac{1}{6}}\right)$ [38], the length of tube needed to create a fully developed turbulent flow is calculated about 30 cm at Reynolds number 40,000 (maximum Reynolds number in this study). Therefore, considering the length of the heat exchanger, 60 cm, it assures that the flow would be developed for all experiments. The outer surface of the test section was thermally insulated by glass wool with 7 cm thickness to minimizing the heat loss to the surrounding.

The nanofluid is placed in a cylindrical 16 L carbon steel reservoir tank (the inner layer is corrosion protected). At the bottom of the tank, an electrical heater with 3 kW power is embedded which is capable of heating the fluid up to the boiling temperature. This heater is connected to a thermostat with temperature control and a digital display (BR6-FDMP4 models with accuracy of ±0.1 °C between −50 and 150 °C) that indicates and controls the temperature of the hot fluid. The required energy is supplied by 220 V electrical heater. After reaching the required temperature, the nanofluid is pumped into the test section by a centrifugal pump (HAPPY Company with the maximum capacity of 35 L min^{-1}, 0.5 hp, and maximum head of 35 m). The fluid

Fig. 3 **a** schematics of the experimental setup: (*1*) inner tube, (*2*) annulus, (*3*) rotameter, (*4*) control valve, (*5*) cold water pump, (*6*) hot water pump, (*7*) cold reservoir tank, (*8*) hot reservoir tank, (*9*) electrical heater, (*10*) differential pressure gauge, (*11*) thermocouples, (*12*) data logger, (*13*) PC, (*14*) PID controller, **b** photograph of the experimental setup
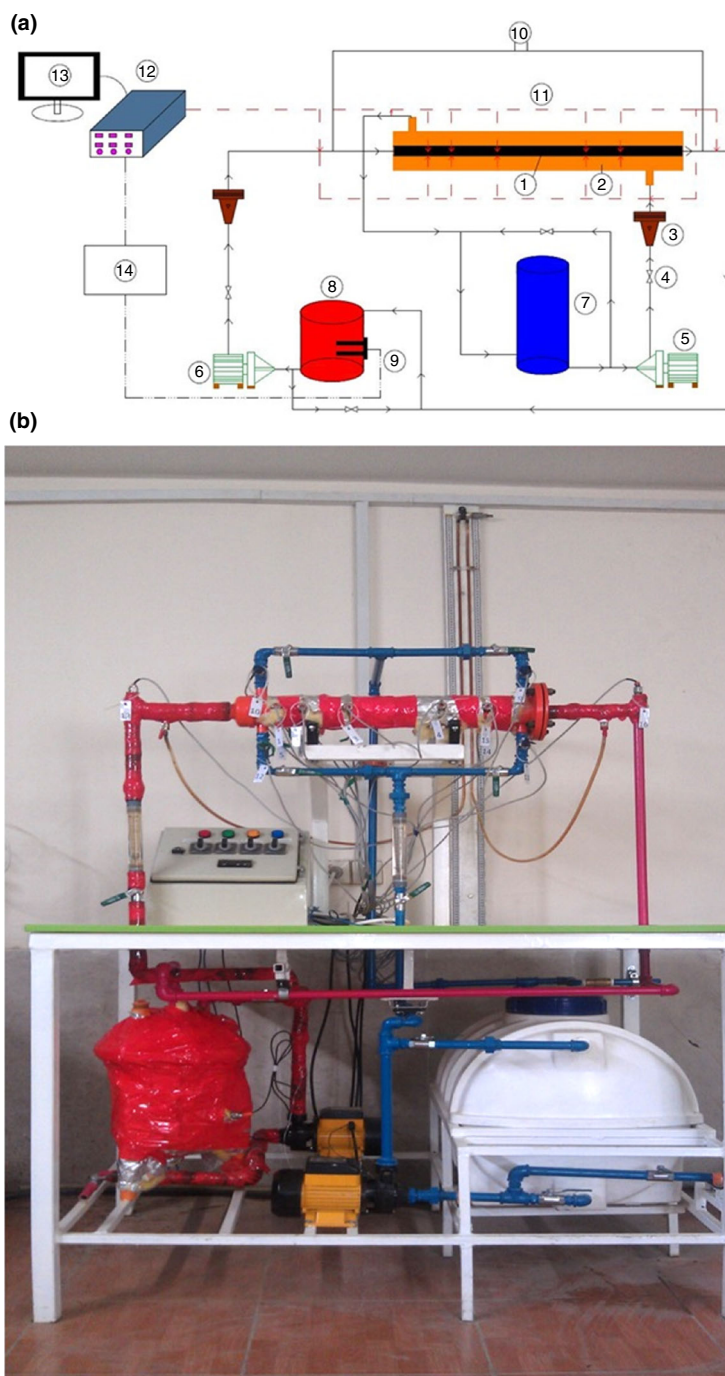
flow can be adjusted by a valve on the recycle line or a valve that is mounted before the flow meter.

Then, the distilled water is poured in the cold cylindrical tank which is made of PVC with capacity of 100 L. It should be noted that the cold reservoir tank temperature was always kept constant at a temperature of 6 °C by a mixture of water and ice. Throughout the test, the cooling fluid flow rate was constant at 13 L min^{-1}. After switching the pump on, the cold fluid passes through the valves. Depending on the experimental

conditions, co-current or countercurrent flow can be prepared in this setup. The specification of cold fluid pump is exactly the same as the hot fluid pump. For measuring flow rates, two flow meters (Technical Groups Model sp.gr.1.0) with operating temperature range between 0 and 90 °C, pressure less than 0.1 MPa, and 1.8–18 L min^{-1} flow rate were used. Precision of the flow meters is 0.1 L min^{-1}. Both flow meters were calibrated by the time taken for a given volume of fluid to be discharged.

Four temperature sensors have been used to measure the bulk temperature of the flow at the inlet and outlet of the inner tube and annulus. So far, major studies on double-tube heat exchangers have calculated the average heat transfer coefficient and thus average Nusselt number. In this study as a novelty, the wall temperature and the bulk temperatures were measured at some points over the length of the heat exchanger to observe the changes in the local convective heat transfer coefficient in the double-tube heat exchanger. For this purpose, eight temperature sensors were located at the distance of 5, 10, 20, and 40 cm from the inlet. Four of them were embedded in the inner tube thickness for measuring the wall temperatures, and four other sensors were inserted inside the inner tube to measure the bulk temperatures. So, the local wall and bulk temperatures can be obtained at four points inside the heat exchanger. The accuracy of all temperature sensors is ±0.1 °C. Data logger (TIKA Company and model TM-1202) was also used for recording the temperature data. All temperature-measuring devices were calibrated before testing. In Fig. 4a, the frontal view or the cross section of the concentric tubes of the heat exchanger is shown. Also in Fig. 4b, the side view of the heat exchanger including the dimensions of the test section and the locations of the embedded temperature sensors is shown.

Uncertainty

The uncertainty analysis was carried out using the procedure proposed by Moffat [39]. Uncertainty of experimental results was determined by measurement deviation of parameters, including flow rate, mass, pressure drop, wall temperature, and fluid bulk temperature. Thereafter, the error of each parameter was incorporated into the estimation of uncertainties.

Flow rate measurement is subjected to two sources of uncertainty: the mass measurement and the time span. Since a precise digital balance was used, the uncertainty related to weighing the fluid can be neglected (±0.01/2000 g). A stopwatch was used to measure the time span of more than 60 s, with maximum human error of ±0.5 s. Thus, the maximum uncertainty of the mass flow rate measurement was ±0.83 %. Uncertainty of temperature measurement using thermometer was ±0.1 °C. Accordingly, the temperature difference had an error of ±0.2 °C. Uncertainty of experimental heat transfer coefficient and friction factor were calculated to be about 9.7 and 4.65 %, respectively. The maximum possible errors for the parameters involved in the analysis are estimated and summarized in Table 3. It must be noted that the estimated uncertainties are based on the manufactures specification and not on a calibration of the instruments.

Data processing

Thermo-physical properties of nanofluids

Addition of nanoparticle in the base fluid will cause changes in its density, specific heat, thermal conductivity, and viscosity. Therefore, before the study on the convective heat transfer performance of the nanofluid, the properties of nanofluid must be known accurately. By assuming that the nanoparticles are well dispersed in the base fluid, the concentration of nanoparticles may be considered uniformly throughout the tube. Although this assumption may not be true in reality because of some physical phenomena such as particle migration, it can be a useful tool to evaluate the physical properties of a nanofluid. In the current research, nanoparticle volume fraction is assumed to be uniform and constant. The greater Brownian diffusion coefficient (less nanoparticle diameter) and less thermophoresis force (lower volumetric concentration) may lead to ignore nanoparticle migration [19–21]. In the present study, nanoparticles diameter is small and nanofluid concentration is low; therefore, the ratio of Brownian diffusion coefficient to the thermophoresis diffusion coefficient (N_{BT}) is high. Therefore, nanoparticle migration can be ignored in this study. Hence, uniform volumetric concentration of nanofluid can be assumed through the heat exchanger.

The following correlation proposed by Pak and Cho [40] is used to estimate the nanofluid density:

$$\rho_{nf} = \varphi\rho_p + (1 - \varphi)\rho_{bf} \tag{1}$$

C_{pnf} is the effective specific heat of the nanofluid which can be calculated from Xuan and Roetzel [41] relation:

$$C_{pnf} = \frac{(1 - \varphi)\rho_{bf}C_{pbf} + \varphi\rho_p C_{pp}}{\rho_{nf}} \tag{2}$$

So far, various theoretical and experimental studies have been conducted and various correlations have been proposed for the dynamic viscosity and thermal conductivity of nanofluids. However, any general correlation has not been established due to the lack of common understanding on the mechanism of nanofluid. The effective dynamic viscosity and thermal conductivity of nanofluid can be usually calculated by existing formulas that have been obtained for two-phase mixtures, i.e., the well-known Einstein equation [42] for dynamic viscosity and the Maxwell model [43] for thermal conductivity. Some previous studies showed the aforementioned correlations are not made for nowadays nanofluids. They have weak approaches which can be employed to characterize the nanofluid's viscosity and thermal conductivity. Therefore, in this study, the viscosity and thermal conductivity of the

Fig. 4 a Frontal view of the double-tube heat exchanger (all dimensions are in mm), **b** Side view of the double-tube heat exchanger and the locations of the embedded temperature sensors
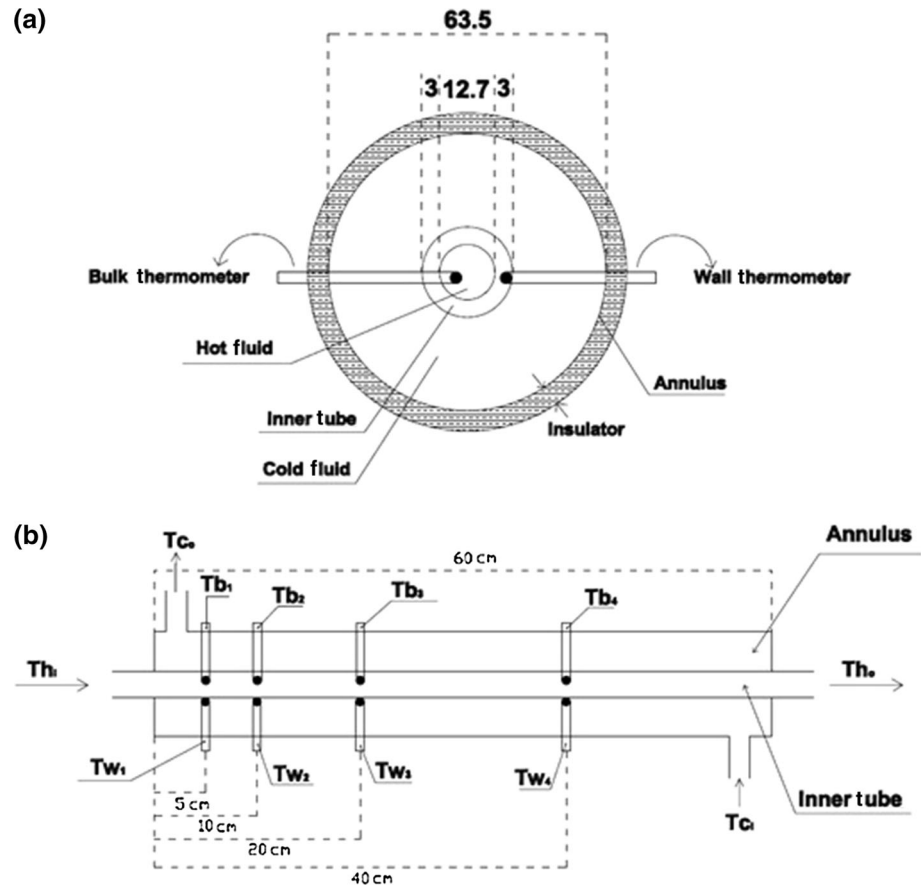

Table 3 Uncertainty of parameters and variables

#	Variable name	Uncertainty error/%
1	Heat transfer coefficient (h)	9.7
2	Reynolds number (Re)	0.83
3	Nusselt number (Nu)	9.7
4	Friction factor (f)	4.65

nanofluid have been obtained from Williams et al. [44] that proposed dynamic viscosity and thermal conductivity equations based on limited experimental data for the γ-Al$_2$O$_3$/water nanofluid.

$$\mu_{\mathrm{nf}} = \mu_{\mathrm{bf}}(T)\exp\left[\frac{4.91\varphi}{(0.2092 - \varphi)}\right] \tag{3}$$

$$k_{\mathrm{nf}} = k_{\mathrm{bf}}(T)(1 + 4.5033\varphi) \tag{4}$$

Data reduction

To calculate the average convective heat transfer coefficient in a double-tube heat exchanger, three different methods were used and each of which faced some

criticism. A new method was presented here to calculate the local and the average heat transfer coefficient in double-tube heat exchangers. In new method, the length of the heat exchanger is divided into some elements. The size of each element calculated such that a pair of the wall and the bulk thermocouples placed exactly in the middle of the element. Since we have four couples of temperature sensors along the heat exchanger, four elements could be considered as shown in Fig. 5. As can be seen, the sizes of the elements are not uniform because more temperature variations occur at the beginning of the heat exchanger. Also, to consider the assumption of constant heat flux in each element, the sizes of the elements should be as small as possible.

Then the inlet and outlet temperatures of each element are calculated using linear interpolation between the experimental temperature data. After calculating the inlet and outlet temperatures of each element, the heat transfer rate and the heat flux can be calculated. In fact, the logic of this approach is that the heat flux is assumed constant for each small element. Finally, using Newton's cooling law, local heat transfer coefficient is calculated for each element, and then, by using Eq. (5) the average heat transfer coefficient can be obtained.

$$h_{av} = \frac{1}{L} \int_0^L h \, dx \qquad (5)$$

Figure 5 shows that 50 of 60 cm of the length of the heat exchanger is covered by four elements. 2.5 cm from the beginning and 7.5 cm from the end of the heat exchanger are not considered in the calculation because of the lack of thermocouples exactly at the inlet and outlet of the heat exchanger. Furthermore, at the end of heat exchanger, due to end effects in some experiments, the heat transfer rate was calculated to be negative; therefore, it is better to neglect the last 7.5 cm from the calculation. On the other hand, because of a very high heat transfer coefficient at the 2.5 cm beginning and a very low heat transfer coefficient at the 7.5 cm end of the heat exchanger, the removal of these two regions has probably no impact on the results as these two effects cancel out each other on the calculation of the average heat transfer coefficient. For more precise calculations, more thermocouples could be embedded in the heat exchanger to have smaller size elements.

Results and discussion

Validation of the experimental data

In order to check the accuracy of the experimental setup, distilled water was used as a working fluid and forced convective heat transfer coefficient and friction factor were measured in turbulent flow regime. The experimental results were compared with the prediction of Gnielinski [45] correlation shown as Eq. (6), and Colebrook equation [46] as Eq. (7):

$$Nu_D = \frac{\left(\frac{f}{8}\right)(Re_D - 1000)Pr}{1 + 12.7\left(\frac{f}{8}\right)^{\frac{1}{2}}\left(Pr^{\frac{2}{3}} - 1\right)} \qquad (6a)$$

$$f = (0.79 \ln Re_D - 1.64)^{-2} \qquad (6b)$$

which is valid in the range $2300 < Re < 5 \times 10^6$ and $0.5 < Pr < 2000$

$$\frac{1}{f^{\frac{1}{2}}} = -2 \times \log\left(\frac{2.51}{Re f^{\frac{1}{2}}} + \frac{\varepsilon/D}{3.7}\right) \qquad (7)$$

where ε is the roughness of the stainless steel 316 tube and equals to 0.002 mm [46].

Figure 6 shows the comparison of the test experimental data of co-current and countercurrent flows with Gnielinski correlation. Absolute average errors of the prediction of Gnielinski correlation are 8 and 33 % for the co-current and countercurrent flow, respectively. It should be remembered that Gnielinski empirical correlation was originally presented for calculating forced convective heat transfer coefficient in turbulent flow regime inside smooth tubes with constant heat flux or constant wall temperature boundary conditions. In this study, however, it is used in double-tube heat exchanger. As a result, this error is somehow inevitable and predictable.

Figure 7 shows the calculated friction factor of distilled water obtained from experiment and the prediction of Colebrook [43] equation at various Reynolds numbers. An absolute average error of the prediction is 8 %. Thus, comparison between the results shows a good agreement with Colebrook equation.

Heat transfer characteristics

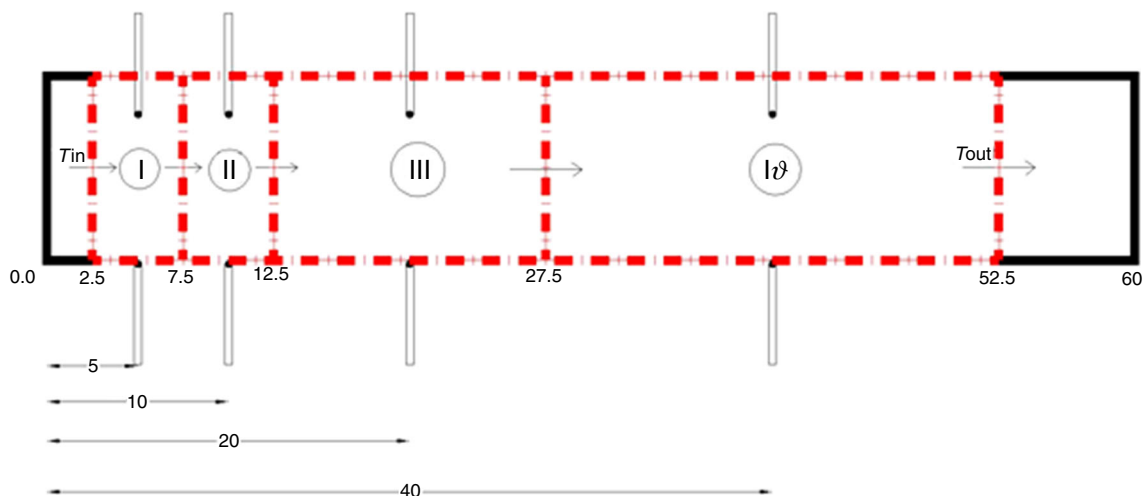As commonly reported in the literature [47, 48], the constant Reynolds number condition has been used for

Fig. 5 Characteristics of elements in the double-tube heat exchanger (all dimensions are in cm)
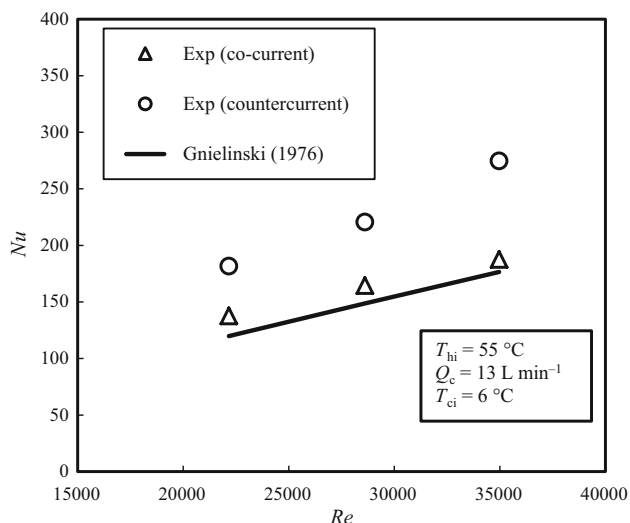
Fig. 6 Comparison between the measured Nusselt Number with the prediction of Gnielinski correlation in co-current and countercurrent flow

Fig. 7 Comparison of the experimental friction factor of distilled water with the prediction of Colebrook equation

comparing heat transfer performance of nanofluids with base fluid. Reynolds number is a function of thermo-physical properties like density and dynamic viscosity. If the thermo-physical properties of the fluid remain constant or same fluid is used, the Reynolds number can be used as the basis of comparison. However, the nanofluids with different volume concentrations have different thermo-physical properties than base fluid. However, substantial reduction in the Reynolds number can be observed at a fixed flow rate, with the increase in concentration of nanoparticles. Results of this study demonstrated that at 0.15 vol% of alumina in base fluid, the Reynolds number decreases by about 4 % as compared to the base fluid. The main reason behind the reduction in Reynolds number can be the increase in viscosity with increasing particle concentration.

Due to the reduction in the Reynolds number at a particular flow rate with small addition of alumina nanoparticles, the Reynolds number cannot be suitable for comparing the convective heat transfer characteristics of nanofluids as compared to the base fluid [49, 50]. Hence, in this study, the heat transfer performance of nanofluids and base fluid was compared at the basis of the constant flow rate instead of the commonly used constant Reynolds number.

Local heat transfer coefficient of the nanofluid

Design and construction of our experimental setup allowed measuring local heat transfer coefficient in the double-tube heat exchanger, which has not been studied before. Figure 8 shows local heat transfer coefficient
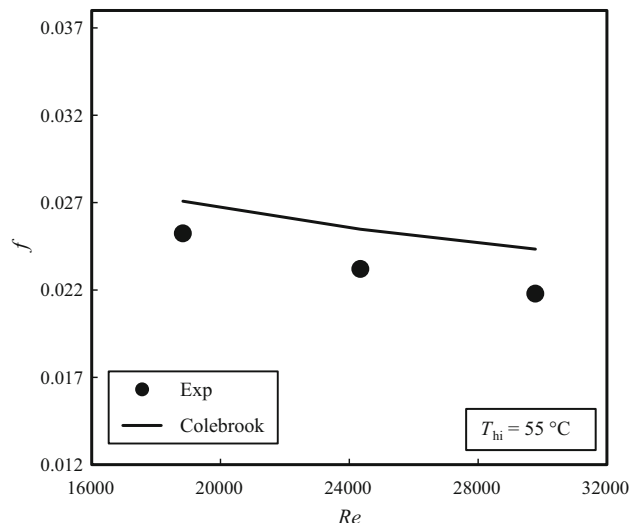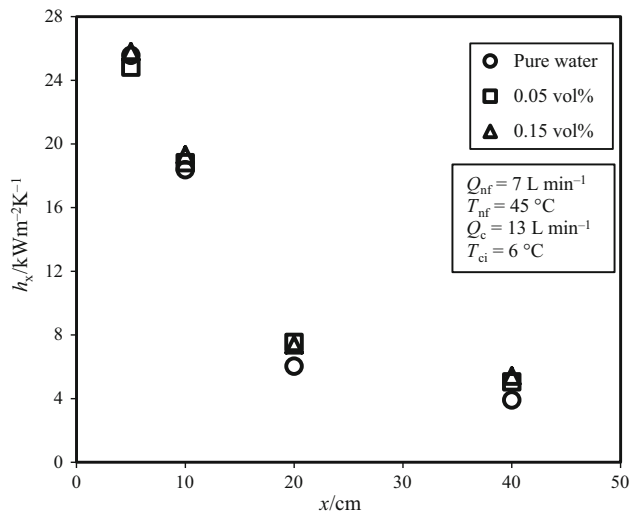

Fig. 8 Local heat transfer coefficient variation of water and nanofluids along axial distance

along the test section for different concentrations of nanofluid and pure water at a constant flow rate and temperature. It shows that the local convective heat transfer coefficient decreases sharply by distancing far from the beginning of the heat exchanger. Since the thermal boundary layer thickness is small at the beginning of the test section, low thermal resistance leads to higher heat transfer coefficient at the beginning of the heat exchanger. The reduction in the local heat transfer coefficient is continued until fully developed region is established. It is also shown in Fig. 8 that the local convective heat transfer coefficient increases with increasing the nanoparticles concentration.
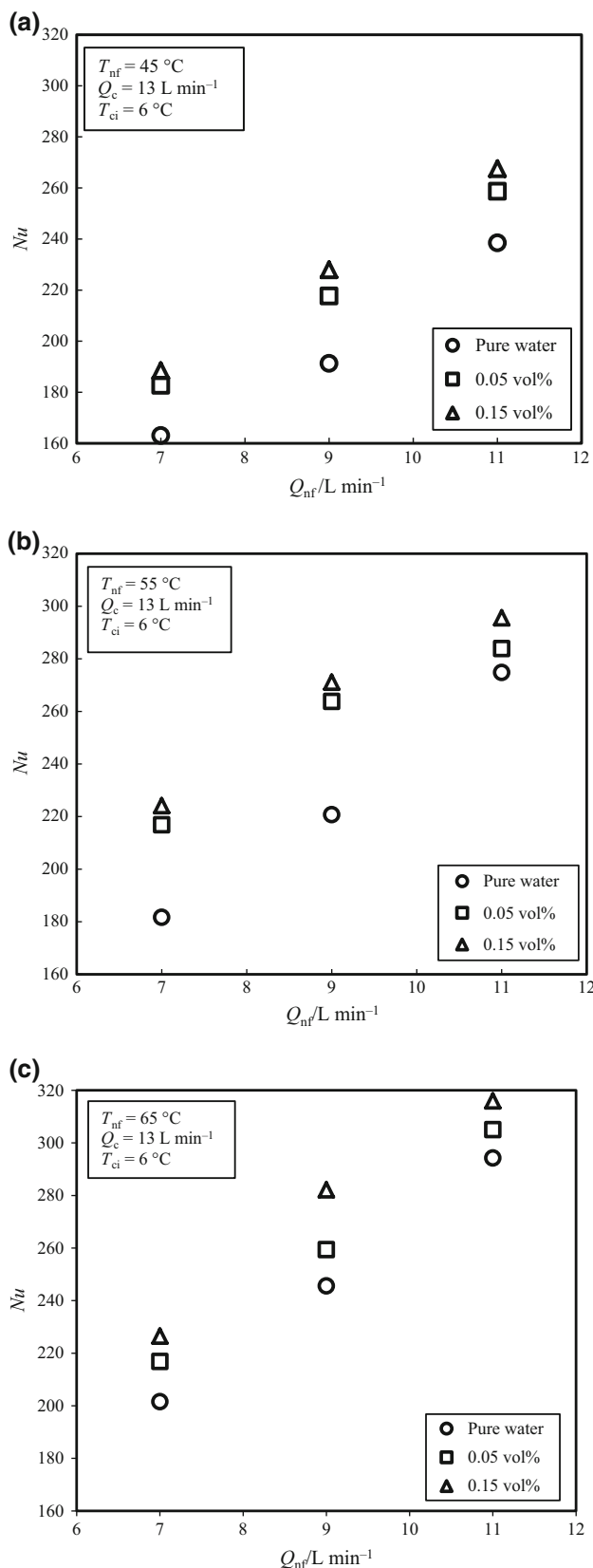
(a)

(b)

(c)

Fig. 9 Variation of average Nusselt number with nanofluid flow rate at the inlet temperatures of **a** 45 °C, **b** 55 °C, and **c** 65 °C
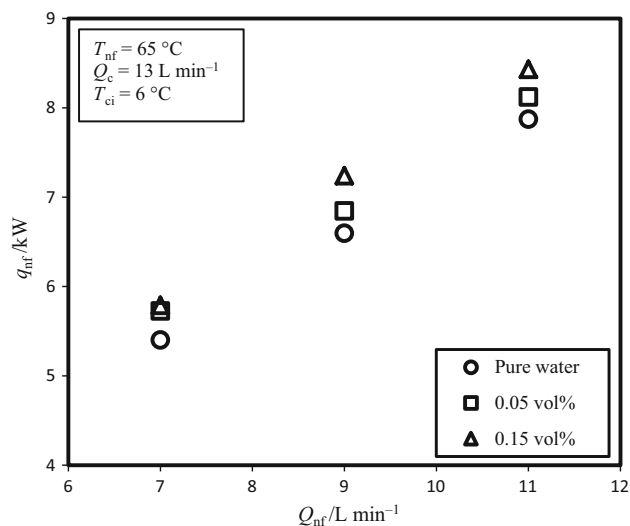

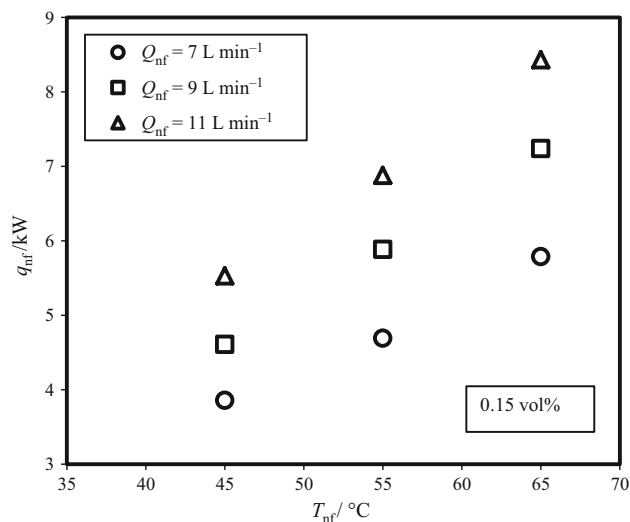**Fig. 10** Nanofluid heat transfer rate versus nanofluid flow rate

Fig. 11 Nanofluid heat transfer rate versus temperature

Average Nusselt number of nanofluids

Figure 9 shows the average Nusselt number for nanofluid and water at different volume fraction, temperature, and flow rate. The results show that nanofluids have higher Nusselt number than base fluid and Nusselt number increases with increasing volume fraction of nanoparticles and nanofluids temperature. In addition, Nusselt number of nanofluids and water increases by increasing the flow rate. Previous researchers mentioned that the reason for heat transfer enhancement of nanofluids included many issues, such as the mixing effects of particles near the wall, thermal conductivity enhancement, Brownian motion of particles, particle migration, and reduction in boundary layer thickness [24, 35].

As shown in Fig. 9, no sensible increase observed in the heat transfer of nanofluids with increasing particle concentrations. For example, at 7 L min^{-1} hot fluid flow rate and 45 °C nanofluids, h_{nf}/h_{bf} parameters are, respectively, 1.12 and 1.16 for 0.05 and 0.15 vol%.

The mentioned last fact was against the observation of Xuan and Li [51] and Heris et al. [52] whom reported a large increase in the heat transfer of a nanofluid with augmentation of the nanoparticles volume fraction. However, the result of this study is consistent with the experimental results reported by Fotukian and Nasr [53], and Sajadi and Kazemi [54]. In addition, by increasing the flow rate of nanofluid, in almost all cases, the heat transfer coefficient ratio (h_{nf}/h_{bf}) is reduced.

Figures 10 and 11 show the effects of nanoparticles concentration, and nanofluid flow rate and temperature on heat transfer rate. The results show that the effect of nanofluid flow rate is greater than the nanofluid's concentration. For example, at 65 °C and 0.15 vol% concentration, average heat transfer rate increases about 9 % than base fluid.

Nusselt number for the fully developed turbulent flow for Al$_2$O$_3$/water nanofluid is compared with the correlation proposed by Pak and Cho [47], Maiga et al. [55], and Xuan and Li [51], which are shown as below, respectively:

$$Nu = 0.021Re^{0.8}Pr^{0.5} \tag{8}$$

$$Nu = 0.085Re^{0.71}Pr^{0.35} \tag{9}$$

$$Nu = 0.0059\left(1 + 7.6286\varphi^{0.6886}Pe_{p}^{0.001}\right)Re_{nf}^{0.9238}Pr_{nf}^{0.4} \tag{10}$$

A comparison carried out between the experimental data and the mentioned correlations. Results show that Maiga correlation shows better coverage to the experimental data. For example, Fig. 12 shows comparison between Maiga correlation and experimental data with 0.15 vol% concentration of nanofluid and 45, 55, and 65 °C hot fluid inlet temperature.

Flow properties of nanofluids

Figure 13 presents the variations of isothermal pressure drop along inner tube as a function of Reynolds number at various concentrations of nanoparticles. As depicted, the pressure drop increases by increasing the concentration of

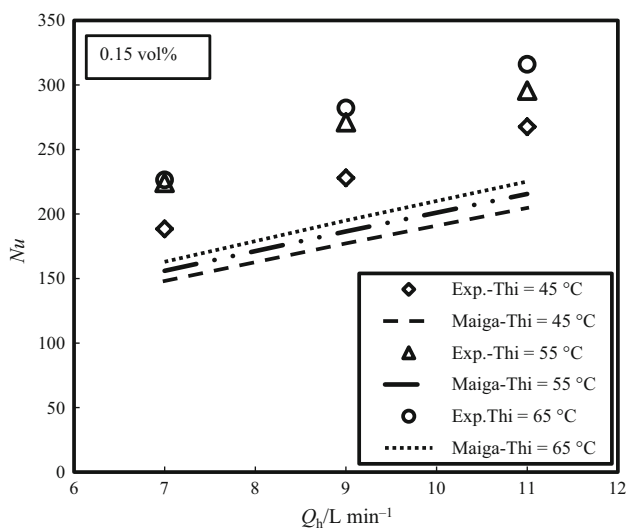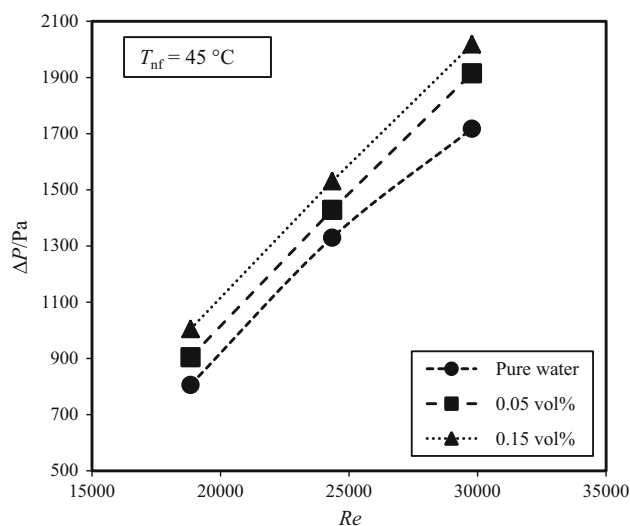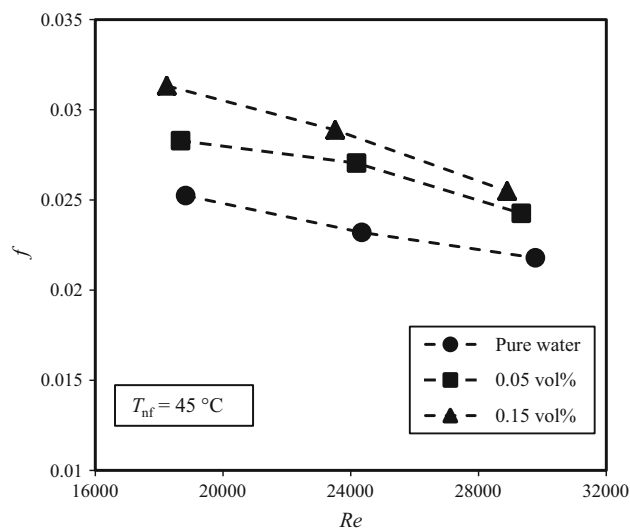**Fig. 13** Variations of pressure drop versus Reynolds number

Fig. 12 Comparison of experimental Nusselt number with existing convective heat transfer correlation at 0.15 vol% in countercurrent flow

Fig. 14 Variations of friction factor versus Reynolds number

Table 4 Experimental data for convective heat transfer and pressure drop at 45 °C

φ/%	Re	h_{bf}/Wm^{-2} K^{-1}	h_{nf}/Wm^{-2} K^{-1}	h_{nf}/h_{bf}	ΔP_{bf}/Pa	ΔP_{nf}/Pa	$\Delta P_{nf}/\Delta P_{bf}$
0.05	18,671	8154.9	9139.4	1.12	805.7	904.2	1.12
0.05	24,182	9568	10,887.4	1.14	1329.7	1428.9	1.07
0.05	29,340	11,928	12,939	1.08	1717.6	1915	1.11
0.15	18,237	8155	9426.7	1.16	805.7	1004.4	1.25
0.15	23,512	9568	11,403.1	1.19	1329.7	1530.9	1.15
0.15	28,895	11,928	13,382.7	1.12	1717.6	2017.9	1.17

nanoparticles due to the rise of the viscosity of working fluid. It is observed that pressure drop is greater at higher Reynolds number where the laminar sublayer is thinner and subsequently the shear stress increases.

Variation of isothermal friction factor versus Reynolds number at various concentrations of nanoparticles is illustrated in Fig. 14. It is shown that the friction factor reduces as the Reynolds number increases. The effects of particle loading on the friction factor are more visible at low Reynolds numbers. At low Reynolds numbers, the friction factor increases with an increase in the volume fraction of nanoparticles. This is due to the fact that at low flow velocities, the ratio of the viscous forces to the inertia forces is greater; therefore, adding the nanoparticles to pure water leads to more increase in shear stress among the fluid layers, and hence, the friction factor increase is more considerable. Maximum enhancement of the friction factor is obtained about 25 % at the nanoparticle concentration of 0.15 vol% and at Reynolds number approximately 18,000. The experimental data are also reported in Table 4.

Conclusions

In the present study, fully developed turbulent flow heat transfer and the pressure drop behavior of γ-Al₂O₃/water nanofluid in a double-tube heat exchanger have been experimentally investigated. Results were provided as Nusselt number, local heat transfer coefficient, heat transfer rate, pressure drop, and friction factor in the heat exchanger. The following conclusions have been drawn from the present study:

- By suspending a small amount of γ-Al₂O₃ nanoparticles, heat transfer coefficient of nanofluids increases. Maximum enhancement of the heat transfer coefficient is 23 % in comparison with pure water which was obtained at 0.15 vol% of γ-Al₂O₃.
- Local convective heat transfer coefficient in double-tube heat exchanger has been measured experimentally for the first time. Results showed that increasing the nanoparticle concentration moderately enhances the local convective heat transfer coefficient.
- Increasing the nanoparticles concentration had not considerable effect on the heat transfer enhancement in the range of concentration studied in this work.
- In almost all cases, the rate of heat transfer coefficient enhancement of nanofluid to that of pure water decreased with increasing the Reynolds number.
- The friction factor of nanofluid increased with increasing the volume fraction of nanoparticles. The maximum friction factor was about 25 % greater than that of pure water which was occurred at the highest volume fraction of nanofluid (0.15 vol%).
- Xuan and Li, Pak and Cho and Maiga correlations underpredicted the Nusselt number of nanofluid. It can be seen that the experimental results obtained in this study were in relatively close agreement with Maiga correlation compared to other correlations.

References

1. Choi SUS, editor. Enhancing thermal conductivity of fluids with nanoparticles. In: Proceedings of the 1995 ASME international mechanical engineering congress and exposition; 1995; New York, USA.
2. Esfe MH, Saedodin S, Yan W-M, Afrand M, Sina N. Study on thermal conductivity of water-based nanofluids with hybrid suspensions of CNTs/Al2O3 nanoparticles. J Therm Anal Calorim. 2016;124(1):455–60.
3. Toghraie D, Chaharsoghi VA, Afrand M. Measurement of thermal conductivity of ZnO–TiO2/EG hybrid nanofluid. J Therm Anal Calorim. 2016;125(1):1–9.
4. Afrand M, Najafabadi KN, Akbari M. Effects of temperature and solid volume fraction on viscosity of SiO 2-MWCNTs/SAE40 hybrid nanofluid as a coolant and lubricant in heat engines. Appl Therm Eng. 2016;102:45–54.
5. Afrand M, Toghraie D, Ruhani B. Effects of temperature and nanoparticles concentration on rheological behavior of Fe 3 O 4– Ag/EG hybrid nanofluid: an experimental study. Exp Therm Fluid Sci. 2016;77:38–44.
6. Eshgarf H, Afrand M. An experimental study on rheological behavior of non-Newtonian hybrid nano-coolant for application in cooling and heating systems. Exp Therm Fluid Sci. 2016;76:221–7.

7. Esfe MH, Afrand M, Karimipour A, Yan W-M, Sina N. An experimental study on thermal conductivity of MgO nanoparticles suspended in a binary mixture of water and ethylene glycol. Int Commun Heat Mass. 2015;67:173–5.

8. Soltanimehr M, Afrand M. Thermal conductivity enhancement of COOH-functionalized MWCNTs/ethylene glycol–water nanofluid for application in heating and cooling systems. Appl Therm Eng. 2016;105:716–23. doi:10.1016/j.applthermaleng.2016.03.089.

9. Xuan Y, Li Q. Investigation on convective heat transfer and flow features of nanofluids. J Heat Transf. 2003;125(1):151–5. doi:10.1115/1.1532008.

10. Yu W, Xie H, Li Y, Chen L, Wang Q. Experimental investigation on the heat transfer properties of Al_2O_3 nanofluids using the mixture of ethylene glycol and water as base fluid. Powder Technol. 2012;230:14–9. doi:10.1016/j.powtec.2012.06.016.

11. Wen D, Ding Y. Experimental investigation into convective heat transfer of nanofluids at the entrance region under laminar flow conditions. Int J Heat Mass Transf. 2004;47(24):5181–8. doi:10.1016/j.ijheatmasstransfer.2004.07.012.

12. Peyghambarzadeh SM, Hashemabadi SH, Jamnani MS, Hoseini SM. Improving the cooling performance of automobile radiator with Al_2O_3/water nanofluid. Appl Therm Eng. 2011;31(10):1833–8. doi:10.1016/j.applthermaleng.2011.02.029.

13. Hosseinipour E, Heris SZ, Shanbedi M. Experimental investigation of pressure drop and heat transfer performance of amino acid-functionalized MWCNT in the circular tube. J Therm Anal Calorim. 2015;. doi:10.1007/s10973-015-5137-4.

14. Tarighaleslami AH, Walmsley TG, Walmsley MR, Atkins MJ, Neale JR. Heat transfer enhancement in heat recovery loops using nanofluids as the intermediate fluid. Chem Eng. 2015;45:991–6.

15. Hosseinzadeh M, Heris SZ, Beheshti A, Shanbedi M. Convective heat transfer and friction factor of aqueous Fe3O4 nanofluid flow under laminar regime. J Therm Anal Calorim. 2016;124(2):827–38.

16. Esfe MH, Saedodin S. Turbulent forced convection heat transfer and thermophysical properties of Mgo–water nanofluid with consideration of different nanoparticles diameter, an empirical study. J Therm Anal Calorim. 2015;119(2):1205–13.

17. Bahiraei M. A numerical study of heat transfer characteristics of CuO–water nanofluid by Euler-Lagrange approach. J Therm Anal Calorim. 2016;123(2):1591–9.

18. El-Maghlany WM, Hanafy AA, Hassan AA, El-Magid MA. Experimental study of Cu–water nanofluid heat transfer and pressure drop in a horizontal double-tube heat exchanger. Exp Therm Fluid Sci. 2016;78:100–11.

19. Malvandi A, Ganji DD. Brownian motion and thermophoresis effects on slip flow of alumina/water nanofluid inside a circular microchannel in the presence of a magnetic field. Int J Therm Sci. 2014;84:196–206. doi:10.1016/j.ijthermalsci.2014.05.013.

20. Malvandi A, Ghasemi A, Ganji D. Thermal performance analysis of hydromagnetic Al_2O_3–water nanofluid flows inside a concentric microannulus considering nanoparticle migration and asymmetric heating. Int J Therm Sci. 2016;109:10–22.

21. Malvandi A, Ganji D. Effects of nanoparticle migration on water/alumina nanofluid flow inside a horizontal annulus with a moving core. J Mech. 2015;31(03):291–305.

22. Hemmat Esfe M, Saedodin S, Mahian O, Wongwises S. Heat transfer characteristics and pressure drop of COOH-functionalized DWCNTs/water nanofluid in turbulent flow at low concentrations. Int J Heat Mass Transf. 2014;73:186–94. doi:10.1016/j.ijheatmasstransfer.2014.01.069.

23. Darzi AAR, Farhadi M, Sedighi K. Heat transfer and flow characteristics of Al_2O_3–water nanofluid in a double tube heat exchanger. Int Commun Heat Mass. 2013;47:105–12. doi:10.1016/j.icheatmasstransfer.2013.06.003.

24. Duangthongsuk W, Wongwises S. An experimental study on the heat transfer performance and pressure drop of TiO_2-water nanofluids flowing under a turbulent flow regime. Int J Heat Mass Transf. 2010;53(1–3):334–44. doi:10.1016/j.ijheatmasstransfer.2009.09.024.

25. Zamzamian A, Oskouie SN, Doosthoseini A, Joneidi A, Pazouki M. Experimental investigation of forced convective heat transfer coefficient in nanofluids of Al_2O_3/EG and CuO/EG in a double pipe and plate heat exchangers under turbulent flow. Exp Therm Fluid Sci. 2011;35(3):495–502. doi:10.1016/j.expthermflusci.2010.11.013.

26. Hemmat Esfe M, Saedodin S, Mahmoodi M. Experimental studies on the convective heat transfer performance and thermophysical properties of MgO–water nanofluid under turbulent flow. Exp Therm Fluid Sci. 2014;52:68–78. doi:10.1016/j.expthermflusci.2013.08.023.

27. Chun B-H, Kang H, Kim S. Effect of alumina nanoparticles in the fluid on heat transfer in double-pipe heat exchanger system. Korean J Chem Eng. 2008;25(5):966–71. doi:10.1007/s11814-008-0156-5.

28. Aghayari R, Maddah H, Ashori F, Hakiminejad A, Aghili M. Effect of nanoparticles on heat transfer in mini double-pipe heat exchangers in turbulent flow. Heat Mass Transfer. 2014;. doi:10.1007/s00231-014-1415-0.

29. Khalifa AJN, Banwan MA. Effect of volume fraction of γ-Al_2O_3 nanofluid on heat transfer enhancement in a concentric tube heat exchanger. Heat Transf Eng. 2015;36(16):1387–96. doi:10.1080/01457632.2015.1003719.

30. Sarafraz MM, Hormozi F. Intensification of forced convection heat transfer using biological nanofluid in a double-pipe heat exchanger. Exp Therm Fluid Sci. 2015;66:279–89. doi:10.1016/j.expthermflusci.2015.03.028.

31. Sergis A, Hardalupas Y. Anomalous heat transfer modes of nanofluids: a review based on statistical analysis. Nanoscale Res Lett. 2011;6(1):391.

32. Fotukian SM, Nasr Esfahany M. Experimental investigation of turbulent convective heat transfer of dilute γ-Al_2O_3/water nanofluid inside a circular tube. Int J Heat Fluid Flow. 2010;31(4):606–12. doi:10.1016/j.ijheatfluidflow.2010.02.020.

33. Ni R, Zhou S-Q, Xia K-Q. An experimental investigation of turbulent thermal convection in water-based alumina nanofluid. Phys Fluids. 2011;23(2):022005. doi:10.1063/1.3553281.

34. Peyghambarzadeh SM, Hashemabadi SH, Naraki M, Vermahmoudi Y. Experimental study of overall heat transfer coefficient in the application of dilute nanofluids in the car radiator. Appl Therm Eng. 2013;52(1):8–16. doi:10.1016/j.applthermaleng.2012.11.013.

35. Kim D, Kwon Y, Cho Y, Li C, Cheong S, Hwang Y, et al. Convective heat transfer characteristics of nanofluids under laminar and turbulent flow conditions. Curr Appl Phys. 2009;9(2, Supplement):e119–23. doi:10.1016/j.cap.2008.12.047.

36. Anoop KB, Sundararajan T, Das SK. Effect of particle size on the convective heat transfer in nanofluid in the developing region. Int J Heat Mass Transf. 2009;52(9–10):2189–95. doi:10.1016/j.ijheatmasstransfer.2007.11.063.

37. Nasiri M, Etemad SG, Bagheri R. Experimental heat transfer of nanofluid through an annular duct. Int Commun Heat Mass Transf. 2011;38(7):958–63. doi:10.1016/j.icheatmasstransfer.2011.04.011.

38. White FM. Viscous fluid flow. 2nd ed. New York: McGraw-Hill, Inc.; 2006.

39. Moffat RJ. Describing the uncertainties in experimental results. Exp Therm Fluid Sci. 1988;1(1):3–17. doi:10.1016/0894-1777(88)90043-X.

40. Pak BC, Cho YI. Hydrodynamic and heat transfer study of dispersed fluids with submicron metallic oxide particles. Exp Heat Transf. 1998;11(2):151–70. doi:10.1080/08916159808946559.

41. Xuan Y, Roetzel W. Conceptions for heat transfer correlation of nanofluids. Int J Heat Mass Transfer. 2000;43(19):3701–7.
42. Einstein A. A new determination of the molecular dimensions. Annphysics. 1906;19(2):289–306.
43. Maxwell JC. A treatise on electricity and magnetism. Oxford: Clarendon Press; 1881.
44. Williams W, Buongiorno J, Hu L-W. Experimental investigation of turbulent convective heat transfer and pressure loss of alumina/water and zirconia/water nanoparticle colloids (nanofluids) in horizontal tubes. J Heat Transf. 2008;130(4):042412.
45. Gnielinski V. New equations for heat and mass-transfer in turbulent pipe and channel flow. Int Chem Eng. 1976;16(2):359–68.
46. White FM. Fluid mechanics. 4th ed. New York: McGraw-Hill, Inc; 2001.
47. Pak BC, Cho YI. Hydrodynamic and heat transfer study of dispersed fluids with submicron metallic oxide particles. Exp Heat Transf Int J. 1998;11(2):151–70.
48. Yu W, France DM, Smith DS, Singh D, Timofeeva EV, Routbort JL. Heat transfer to a silicon carbide/water nanofluid. Int J Heat Mass Transf. 2009;52(15–16):3606–12. doi:10.1016/j.ijheatmasstransfer.2009.02.036.
49. Yu W, France D, Timofeeva E, Singh D, Routbort J. Thermophysical property-related comparison criteria for nanofluid heat transfer enhancement in turbulent flow. Appl Phys Lett. 2010;96(21):213109.
50. Yu W, France DM, Timofeeva EV, Singh D, Routbort JL. Comparative review of turbulent heat transfer of nanofluids. Int J Heat Mass Transf. 2012;55(21):5380–96.
51. Xuan Y, Li Q. Heat transfer enhancement of nanofluids. Int J Heat Fluid Flow. 2000;21(1):58–64. doi:10.1016/S0142-727X(99)00067-3.
52. Heris SZ, Esfahany MN, Etemad SG. Experimental investigation of convective heat transfer of Al$_2$O$_3$/water nanofluid in circular tube. Int J Heat Fluid Flow. 2007;28(2):203–10.
53. Fotukian SM, Nasr Esfahany M. Experimental study of turbulent convective heat transfer and pressure drop of dilute CuO/water nanofluid inside a circular tube. Int Commun Heat Mass. 2010;37(2):214–9. doi:10.1016/j.icheatmasstransfer.2009.10.003.
54. Sajadi AR, Kazemi MH. Investigation of turbulent convective heat transfer and pressure drop of TiO2/water nanofluid in circular tube. Int Commun Heat Mass. 2011;38(10):1474–8. doi:10.1016/j.icheatmasstransfer.2011.07.007.
55. Maïga SEB, Palm SJ, Nguyen CT, Roy G, Galanis N. Heat transfer enhancement by using nanofluids in forced convection flows. Int J Heat Fluid Flow. 2005;26(4):530–46. doi:10.1016/j.ijheatfluidflow.2005.02.004.